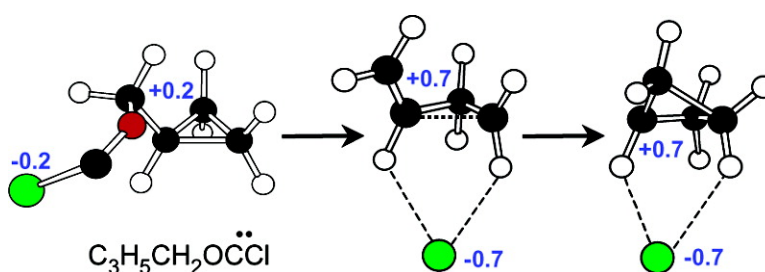


Rearrangements Concerted with Fragmentation of Cyclopropylmethoxychlorocarbene and Cyclobutoxychlorocarbene in Hydrocarbon Solvents and Ar Matrices

Robert A. Moss, Ronald R. Sauers, Fengmei Zheng, Xiaolin Fu, Thomas Bally, and Alexander Maltsev

J. Am. Chem. Soc., 2004, 126 (27), 8466-8476 • DOI: 10.1021/ja049421x • Publication Date (Web): 19 June 2004

Downloaded from <http://pubs.acs.org> on March 31, 2009



More About This Article

Additional resources and features associated with this article are available within the HTML version:

- Supporting Information
- Access to high resolution figures
- Links to articles and content related to this article
- Copyright permission to reproduce figures and/or text from this article

[View the Full Text HTML](#)

Rearrangements Concerted with Fragmentation of Cyclopropylmethoxychlorocarbene and Cyclobutoxychlorocarbene in Hydrocarbon Solvents and Ar Matrices

Robert A. Moss,^{*,†} Ronald R. Sauers,^{*,†} Fengmei Zheng,[†] Xiaolin Fu,[†] Thomas Bally,^{*,‡} and Alexander Maltsev[‡]

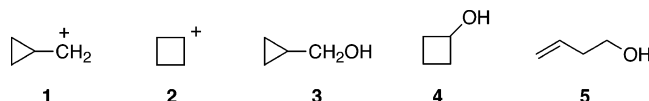
Contribution from the Department of Chemistry and Chemical Biology, Rutgers, The State University of New Jersey, New Brunswick, New Jersey 08903, and Department of Chemistry, University of Fribourg, P erolles, CH-1700 Fribourg, Switzerland

Received February 2, 2004; E-mail: moss@rutchem.rutgers.edu; thomas.bally@unifr.ch

Abstract: Fragmentations of cyclopropylmethoxychlorocarbene (**6**) and cyclobutoxychlorocarbene (**10**) lead to rearrangements that afford mixtures of cyclopropylmethyl chloride (**7**), cyclobutyl chloride (**8**), and 3-butenyl chloride (**9**). Isotopic substitution studies show that these rearrangements are accompanied by partial exchange of the methylene groups within **6** and **10**. Surprisingly, these processes that are typical of carbocations persist in hydrocarbon solvents such as pentane and cyclohexane-*d*₁₂. Quantum chemical calculations reveal that the *cis*-conformers of the incipient oxychlorocarbenes C₄H₇O C Cl decay to C₄H₇Cl + CO via transient hydrogen bonded C₄H₇^{δ+}...Cl^{δ-} complexes which possess significant ion pair character, even in the gas phase or in nonpolar solvents. In contrast to benzyloxychlorocarbene, no free radicals are formed upon generation or photolysis of **6** or **10** in Ar matrixes, although acid chlorides (the recombination products of these radical pairs) are observed. The IR spectra obtained in these experiments show the presence of several conformers of the two C₄H₇O C Cl.

Introduction

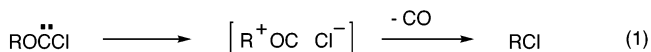
In aqueous solution, the cyclopropylmethyl (**1**) and cyclobutyl (**2**) cations interconvert by rapid 1,2-C shifts which also scramble the methylene carbon atoms within each cation.^{1–3} Thus, aqueous nitrous acid deamination of either cyclopropylmethylamine or cyclobutylamine affords (via the corresponding alkyldiazonium ions, and then **1** and **2**) cyclopropylmethanol (**3**), cyclobutanol (**4**), and 3-butenol (**5**) in a distribution of 52:44:4.^{2,4}



In moderately polar solvents, however, analogous reactions proceed via ion pairs, rather than solvent-equilibrated carbocations, so that the product distributions become precursor dependent. For example, reaction of cyclopropyldiazomethane with ethereal benzoic acid affords [RN₂⁺-O₂CPh], and then [R⁺-O₂CPh], leading to a mixture of the benzoate esters of alcohols **3**, **4**, and **5**, but in a distribution of ~79:14:7.⁴ The

cyclopropylmethyl/cyclobutyl ratio increases from ~1.2 in the aqueous HNO₂ deamination reaction to ~5.8 in the ion pair process, where the products display increased “memory” of their origin. In a related result, the esters formed from reaction of diazocyclobutane with *p*-phenylazobenzoic acid in 98:2 toluene/ethanol give a cyclopropylmethyl/cyclobutyl ratio of 1.3,⁵ much decreased from the ratio of 5.8 found in the cyclopropyldiazomethane/benzoic acid reaction, and featuring a greater cyclobutyl component.

These deaminative processes, which presumably involve ion pairs, are mimicked by the corresponding fragmentation reactions of alkoxychlorocarbenes (eq 1).⁶



Specifically, fragmentation of cyclopropylmethoxychlorocarbene (**6**) in MeCN at 25 °C affords cyclopropylmethyl chloride (**7**), cyclobutyl chloride (**8**), and 3-butenyl chloride (**9**) in a distribution of 73.3:17.1:9.6 (cyclopropylmethyl/cyclobutyl = 4.3), whereas the fragmentation of cyclobutoxychlorocarbene (**10**) yields the same chlorides in a distribution of 55.3:34.3:10.3 (cyclopropylmethyl/cyclobutyl = 1.6); see Scheme 1.⁷

The similarity of these product ratios to those of the corresponding diazoalkane/carboxylic acid processes is clear (5.8

[†] Rutgers University.

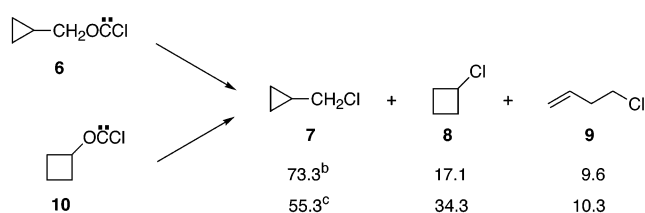
[‡] University of Fribourg.

- (1) Mazur, R. H.; White, W. N.; Seminow, D. A.; Lee, C. C.; Silver, M. S.; Roberts, J. D. *J. Am. Chem. Soc.* **1959**, *81*, 4390.
 (2) Renk, E.; Roberts, J. D. *J. Am. Chem. Soc.* **1961**, *83*, 878.
 (3) Lowry, T. H.; Richardson, K. S. *Mechanism and Theory in Organic Chemistry*, 3rd ed.; Harper and Row: New York, 1987; pp 454–463.
 (4) Moss, R. A.; Shulman, F. C. *Tetrahedron* **1968**, *24*, 2881.

(5) Applequist, D. E.; McGreer, D. E. *J. Am. Chem. Soc.* **1960**, *82*, 1965.

(6) Moss, R. A. *Acc. Chem. Res.* **1999**, *32*, 969.

(7) Moss, R. A.; Zheng, F.; Johnson, L. A.; Sauers, R. R. *J. Phys. Org. Chem.* **2001**, *14*, 400.

Scheme 1^a

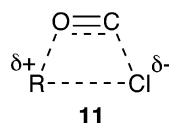
^a In MeCN at 25 °C; carbenes generated by photolysis of the appropriate diazirine precursor. ^bDistribution from **6**. ^cDistribution from **10**.

from RN₂⁺O₂CPh and 4.3 from RO \ddot{C} Cl, when R = cyclopropylmethyl, vs 1.3 and 1.6, respectively, when R = cyclobutyl).

Additional similarities between the product distributions from alkoxychlorocarbene fragmentations and diazonium ion decompositions appear in the menthyl and neomenthyl systems.⁸ Further cases of 1,2-rearrangements associated with alkoxychlorocarbene fragmentations include the 1-norbornylmethyl⁹ and the 2,2-diphenylethyl¹⁰ systems.

Although ion pairs are reasonable intermediates and product precursors from RO \ddot{C} Cl in polar solvents, they are believed to be too energetic to form in hydrocarbon solvents where effective solvation of the ions is absent.¹¹ Nevertheless, we find that alkoxychlorocarbenes fragment just as efficiently in benzene and pentane; examples include RO \ddot{C} Cl with R = benzyl, cyclohexyl, and 1-octyl.¹¹ It should be noted that B3LYP/6-31G* intrinsic reaction coordinate calculations of the fragmentations of carbenes **6** and **10** support the formation of ion pairs from the carbenes.⁷ This raises the question of how these reactions occur.

With fully heterolytic cleavage to cation/anion-CO assemblies precluded in nonpolar solvents, homolytic fragmentation of RO \ddot{C} Cl via [R \cdot ...OC \cdot Cl] and then [R \cdot ...OC...Cl], and concerted fragmentation, via generalized transition state **11**, are alternative mechanisms with computational support.¹¹ There is



spectroscopic evidence that the fragmentation of PhCH₂O \ddot{C} Cl in argon matrices at 12 K leads, in part, to benzyl radicals and \cdot COCl.¹¹ In addition we showed that the fragmentation of *p*-nitrobenzyloxychlorocarbene in dichloroethane (where the *p*-nitro substituent disfavors benzyl cation-chloride anion pairs) proceeds through a transition state with benzyl radical character.¹²

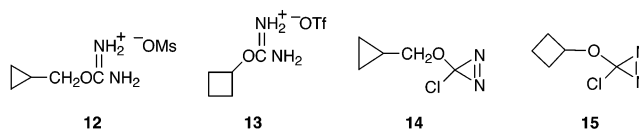
The cyclopropylmethyl system self-indicates its electronic character: cation **1** mainly gives cyclopropylmethyl and cyclobutyl products by 1,2-C rearrangements,¹⁻³ whereas the cyclopropylmethyl radical readily opens to the 3-butenyl radical and associated products.¹³⁻¹⁵ In polar organic solvents, ring opening is minor (Scheme 1) and ionic processes appear dominant,^{7,16} but generation of carbene **6** by flash vacuum

pyrolysis of its precursor diazirine at 365 °C leads to fragmentation with 34% ring opening, which may indicate the involvement of the cyclopropylmethyl radical.¹⁷

What happens in pentane at ambient temperature? We recently noted that “preliminary experiments with cyclopropylmethoxychlorocarbene and cyclobutoxychlorocarbene indicate that the fragmentation and alkyl group rearrangements that afford mixtures of chlorides [7–9] in acetonitrile and dichloroethane persist in pentane. Given the unlikely intervention of classical ion pairs in the latter solvent, deep-seated concerted rearrangements must be coupled with the fragmentations of the carbenes.”¹¹ Here we present experimental and computational studies of the fragmentations of carbenes **6** and **10** in apolar environments, studies that illuminate these unexpectedly persistent rearrangements.

Results and Discussion

Solution Studies. Cyclopropylmethanol and cyclobutanol were converted to the isouronium salts **12** and **13** by reaction in THF with cyanamide and methanesulfonic acid or trifluoromethanesulfonic acid, respectively.^{7,16,18} Conversion of these salts to 3-alkoxy-3-chlorodiazirines **14** and **15** was readily accomplished by reaction with 12% aqueous sodium hypochlorite (“pool chlorine”), saturated with NaCl, in DMSO.^{7,16,19}



These diazirines, which we had previously prepared,^{7,16} can be deazotated to the carbenes **6** or **10** either by photolysis at >320 nm or by keeping them in the dark at room temperature over 1 day. Under both conditions and in MeCN or hydrocarbon solvents, chlorides **7–9** were obtained from both carbenes; product distributions, as determined by capillary GC (photolysis) or NMR (thermolysis), appear in Table 1. These results show that the relative yields of **7–9** do not depend much on the mode of decomposition of the diazirines, which suggests that diazirine excited states are not important product-forming intermediates.

The product distributions for fragmentation in MeCN recorded in Table 1 are in very good agreement with the previously reported data; see Scheme 1.⁷ The low yields of **9**, normally a signature product of the cyclopropylmethyl radical,^{13,14} cannot originate from this species in the present case, because **9** is formed *both* from **6** and from **10**. While formation, followed by ring opening, of the cyclopropylmethyl radical may be possible in the case of carbene **6**, the cyclobutyl radical which would arise by homolysis of **10** is known to be stable toward rearrangement and ring-opening¹⁴ and cannot therefore be the origin of **9**. In contrast, the differing product distributions from **6** or **10** are consistent with polar fragmentations that transit tight but distinct [R⁺ OC Cl⁻] ion pairs.^{6,7}

- (8) Moss, R. A.; Johnson, L. A.; Kacprzyński, M.; Sauer, R. R. *J. Org. Chem.* **2003**, *68*, 5114.
 (9) Moss, R. A.; Zheng, R.; Fedé, J.-M.; Sauer, R. R. *Org. Lett.* **2002**, *4*, 2341.
 (10) Moss, R. A.; Ma, Y. *Tetrahedron Lett.* **2001**, *42*, 6045.
 (11) Moss, R. A.; Ma, Y.; Zheng, F.; Sauer, R. R.; Bally, T.; Maltsev, A.; Toscano, J. P.; Showalter, B. M. *J. Phys. Chem. A* **2002**, *106*, 12280.
 (12) Moss, R. A.; Ma, Y.; Sauer, R. R. *J. Am. Chem. Soc.* **2002**, *124*, 13968.

- (13) Kochi, J. K.; Krusic, P. J.; Eaton, D. R. *J. Am. Chem. Soc.* **1969**, *91*, 1877.
 (14) Sheldon, R. A.; Kochi, J. K. *J. Am. Chem. Soc.* **1970**, *92*, 4395, 5175.
 (15) Newcomb, M.; Glenn, A. G. *J. Am. Chem. Soc.* **1989**, *111*, 275. Ring opening of the cyclopropylmethyl radical to the 3-butenyl radical occurs with $k = 1 \times 10^3 \text{ s}^{-1}$ at 25 °C in THF.
 (16) Moss, R. A.; Ho, G. J.; Wilk, B. K. *Tetrahedron Lett.* **1989**, *30*, 2473.
 (17) Blake, M. E.; Jones, M., Jr.; Zheng, F.; Moss, R. A. *Tetrahedron Lett.* **2002**, *43*, 3069.
 (18) Moss, R. A.; Kaczmarczyk, G. M.; Johnson, L. A. *Synth. Commun.* **2000**, *30*, 3233.
 (19) Graham, W. H. *J. Am. Chem. Soc.* **1965**, *87*, 4396.

Table 1. Product Distributions (%)^a from Cyclopropylmethoxychlorocarbene (**6**) and Cyclobutoxychlorocarbene (**10**)

carbene	solvent	method ^b	c-C ₃ H ₅ CH ₂ Cl (7)	c-C ₄ H ₇ Cl (8)	CH ₂ =CHCH ₂ CH ₂ Cl (9)
6	MeCN	photo	71	19	10
	MeCN	thermal	78	15	7
	pentane	photo	78	12	10
	CH- <i>d</i> ₁₂ ^c	thermal	82	11	7
10	MeCN	photo	55	35	10
	MeCN	thermal	52	33	15
	pentane	photo	60	29	11
	CH- <i>d</i> ₁₂ ^c	thermal	59	30	11

^a Product percentages refer to the total product, excluding products of HCl elimination (C₄H₆) and carbene-HCl adducts (ROCHCl₂). ^b Photo: diazirine precursors **14** and **15** were photolyzed at 25 °C with analysis by GC. Thermal: diazirine precursors were decomposed by storing them for 1 day at room temperature in the dark; analysis is by NMR. ^c Cyclohexane-*d*₁₂.

Strikingly, the product distributions from either carbene vary little when the solvent is changed from MeCN to pentane. Because classical ion pair intermediates are most unlikely in pentane,¹¹ we suggest that the rearranged chlorides from either **6** or **10** in pentane must be formed concertedly with the carbene fragmentations. In the section on computational studies (below), we will describe appropriate pathways for such concerted fragmentation and rearrangement.

Further insight was obtained by labeling carbene **6**. Reduction of methyl cyclopropanecarboxylate with LiAlD₄ gave cyclopropylmethanol- α,α -*d*₂, which was converted first to **12**- α,α -*d*₂, and then to diazirine **14**- α,α -*d*₂ by the procedures described above. The diazirine was irradiated in cyclohexane-*d*₁₂, and the resulting mixture of deuterated chlorides **7**–**9** was analyzed by 400 MHz ¹H NMR spectroscopy. The product distribution was obtained from the integral ratios of the tertiary CH protons of **7** (1.23 ppm) and **8** (4.37 ppm) and the C3-vinyl proton of **9** (5.83 ppm).^{20–22} In two separate experiments, the **7**:**8**:**9** distributions (%) were found to be 75:13:12 and 71:18:11, in reasonable agreement with the GC-determined product distribution from the fragmentation of unlabeled **6** in pentane (Table 1).

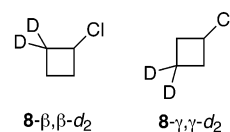
Analysis of the label distributions in products **7** and **8** could also be carried out from the NMR spectrum of the mixture. For **7**, appearance of the α -CH₂ doublet at 3.44 ppm (integral weight 2.07), in comparison to the β -CH at 1.23 ppm (integral weight 4.98, representing both **7**- α,α -*d*₂ and **7**- α,α -*h*₂), indicates an α -CH₂/ α -CD₂ distribution of ~21:79. Complete scrambling of the three methylene groups of **6**- α,α -*d*₂ would afford α -CH₂/ α -CD₂ = 66:33, so that the observed result corresponds to ~32% scrambling. A second experiment gave a distribution of ~24:76, corresponding to 36% scrambling.

Interestingly, the extent of methylene scrambling in the formation of cyclopropylmethyl chloride (**7**) upon fragmentation of carbene **6**- α,α -*d*₂ in cyclohexane-*d*₁₂ is similar to that observed earlier for the fragmentation in CD₃CN (27–36%).¹⁶ The similarity of both product and label distributions in both hydrocarbon solvents and MeCN may be coincidental or may suggest a similarity of mechanism.

Simple primary RO \ddot{C} Cl (R = *n*-C₄H₉, *n*-C₈H₁₇) avoid unimolecular fragmentation with formation of a primary alkyl

cation as a component of an ion pair. Rather, they serve as substrates for chloride-induced S_N2 fragmentations.^{11,23} Primary RO \ddot{C} Cl whose resulting carbocations R⁺ are stabilized, such as PhCH₂O \ddot{C} Cl and **6**, are more likely to fragment unimolecularly and heterolytically in polar solvents, and PhCH₂O \ddot{C} Cl does indeed appear to do so,¹¹ at least in the absence of carbocation-destabilizing electron-withdrawing substituents on the phenyl group.¹² For carbene **6** in MeCN, prior experimental and computational studies are consistent with ion pair intermediates for fragmentation in polar solvents.^{7,16} The present product and labeling studies for the fragmentation of **6** in hydrocarbon solvents suggest the possibility that concerted fragmentation–rearrangement (see below) might also occur in MeCN. The mechanisms available for the fragmentation of primary RO \ddot{C} Cl are delicately balanced between concerted,¹¹ ionic,^{7,16} and radical^{11,17} pathways. In any given case, the modulation of structure, substituent, or solvent can affect the mechanism that is actually selected.

An NMR study of the cyclobutyl chloride product (**8**) from the fragmentation of **6**- α,α -*d*₂ in cyclohexane-*d*₁₂ also afforded its label distribution. From the integral weights of the β and γ protons of **8** (2.24–2.35, 2.43–2.55 ppm and 1.73–1.85, 1.94–2.03 ppm, respectively), we determined the **8**- β,β -*d*₂ to **8**- γ,γ -*d*₂ distribution as 81:19 (a second experiment gave an identical result). Whatever concerted fragmentation–rearrangement mechanisms are available to carbene **6**, the α,α -*d*₂ label finds its way to both the β and the γ positions of the ring-expanded chloride **8**. Since complete scrambling would make **8**- β,β -*d*₂ 33% of the product mixture, we conclude that **8** is ~58% “scrambled.”



Matrix Isolation Studies. Based on the pioneering studies of Kesselmayer and Sheridan on methoxy-^{24,25} and phenoxychlorocarbenes,²⁶ and our own previous work on benzyloxychlorocarbene,¹¹ we investigated the fate of diazirines **14** and **15** upon photolysis in Ar matrices.

Traces a and b in Figure 1 show the changes observed in the UV/vis spectra on 365 nm photolysis of the two diazirines in Ar at 10 K. In both cases, one can see the decrease of the diazirine bands at 350–370 nm and the increase of a band peaking at ca. 315 nm which appears to be typical for oxychlorocarbenes.^{11,25,26} Prolonged irradiation at 365 nm leads to slow decomposition of the carbenes (which appear to absorb very weakly at this wavelength). In contrast, subsequent irradiation at 313 nm leads to rapid bleaching of this band (traces c and d) whereby no new absorptions appear above 250 nm.

The central part of Figure 2 shows a section of the IR difference spectra that corresponds to the same sequence of irradiations. The decreasing peaks in the red traces a and c correspond to the IR bands of diazirines **14** and **15**, respectively, while the bands that point up in these two traces but point down in the blue traces b and d must be assigned to the oxychloro-

(20) Hrubiec, R. T.; Smith, M. B. *J. Org. Chem.* **1984**, *49*, 431.

(21) Lee, C. C.; Cessna, A. J. *Can. J. Chem.* **1980**, *58*, 1075.

(22) Dupont, A. C.; Audia, V. H.; Waid, P. P.; Carter, J. P. *Synth. Commun.* **1990**, *20*, 1011.

(23) Moss, R. A.; Johnson, L. A.; Merrer, D. C.; Lee, G. E., Jr. *J. Am. Chem. Soc.* **1999**, *121*, 5940.

(24) Sheridan, R. S.; Kesselmayer, M. A. *J. Am. Chem. Soc.* **1984**, *106*, 436.

(25) Kesselmayer, M. A.; Sheridan, R. S. *J. Am. Chem. Soc.* **1986**, *108*, 99.

(26) Kesselmayer, M. A.; Sheridan, R. S. *J. Am. Chem. Soc.* **1986**, *108*, 844.

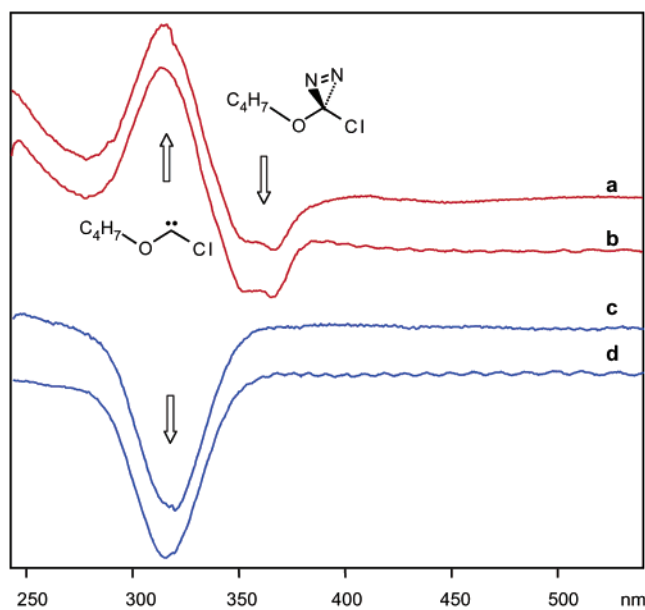


Figure 1. Changes in the UV spectra on deazotization of diazirines **14** (a) and **15** (b) at 365 nm and upon subsequent bleaching of the resulting oxchlorocarbenes **6** (c) and **10** (d).

carbenes **6** and **10**, respectively, that arise as the primary photoproducts. Next to those peaks, one can also discern in the IR spectra the bands of CO (2143 cm^{-1}) and of a $\text{C}_4\text{H}_7\text{COCl}$ around 1820 cm^{-1} which grow strongly during the decomposition of diazirines **14** and on bleaching of the oxchlorocarbene **6**, but much less in the case of **15/10**, thus indicating that homolysis is a less favored photofragmentation pathway in the latter case.

However, in contrast to benzyloxychlorocarbene,¹¹ no trace of the very intense 1877 cm^{-1} peak of the COCl radical²⁷ appeared in any of the present Ar matrix experiments; hence no C_4H_7 radicals are formed from $\text{C}_4\text{H}_7\text{O}\ddot{\text{C}}\text{Cl}$ under these conditions. Apparently, any $\text{R}\cdot\cdots\text{OC}\cdot\text{Cl}$ radical pairs that may be generated recombine immediately to form R-COCl if the radical $\text{R}\cdot$ is not specially stabilized/delocalized. The absence of C_4H_7 radicals might also be due to the availability of a direct photochemical $\text{RO}\ddot{\text{C}}\text{Cl} \rightarrow \text{RCOCl}$ rearrangement pathway in the case of **6** and/or to a partial charge separation in the above radical pairs, which may suffice to allow for spontaneous decay of $\cdot\text{COCl}$.²⁸

Due to the weakness of the IR bands of the chlorides **7–9**, and their partial coincidence with those of the diazirines or the C_4H_7 oxchlorocarbenes, it is impossible to assess the ratio of these three chlorides as they appear under the conditions of the above experiments. Also, a full assignment of the IR spectra of the C_4H_7 oxchlorocarbenes turns out to be very difficult due to the presence of numerous conformers (see computational study). However, it appears, especially from the section of the IR spectra between 1200 and 1400 cm^{-1} , that in the IR difference spectra obtained from **14** and **15** many similar peaks occur, albeit with different relative intensities, which would seem to indicate some crossover between the cyclobutyl and the cyclopropylmethyl species. We will return to this point after discussing the results of our computational studies.

Computational Studies. A. Gas Phase: As pointed out above, one of the complications in the present case is posed by

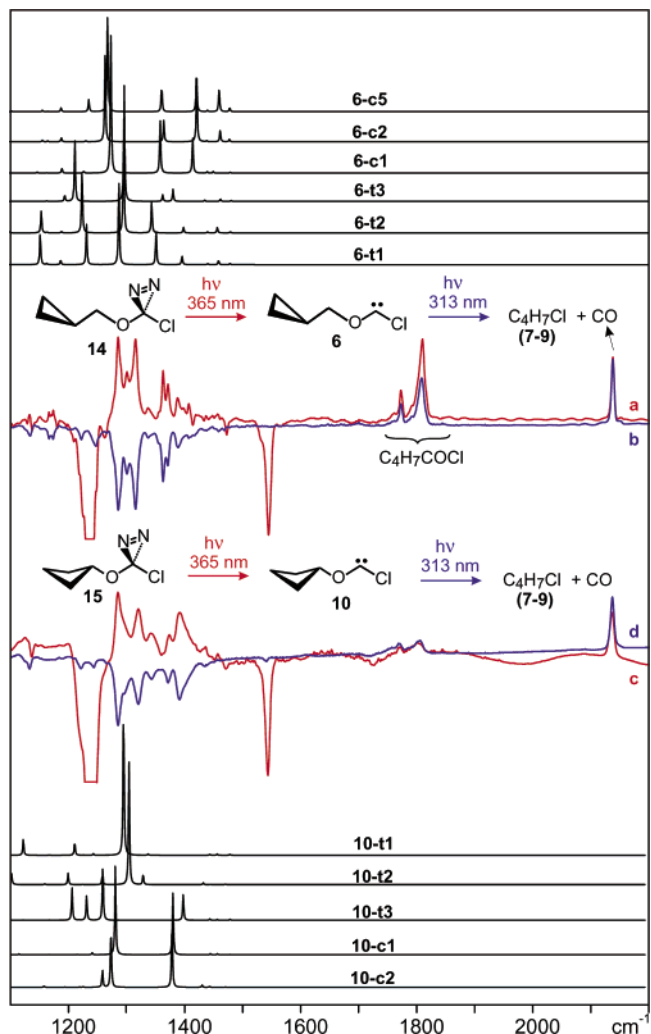


Figure 2. Red and blue traces: changes in the IR spectra on deazotization of diazirines **14** (a) and **15** (c) at 365 nm and upon subsequent bleaching of the resulting oxchlorocarbenes **6** (b) and **10** (d). Black traces: IR spectra of different conformers of oxchlorocarbenes **6** (top) and **10** (bottom). For discussion, see text.

the many possible conformers of the two $\text{C}_4\text{H}_7\text{O}\ddot{\text{C}}\text{Cl}$ species. Thus we began our computational study with an exploration of the potential surfaces comprising these conformers and their interconversion pathways. The corresponding results are displayed in Figures 3 (carbene **6**) and 4 (carbene **10**), while detailed numerical results are given in the Supporting Information. These results show that at room temperature there is rapid equilibration among the different *cis*- and the *trans*-conformers of **6** and **10**, whereby the *trans*-conformers dominate in both oxchlorocarbenes. We also calculated systematically all transition states for *cis* \rightarrow *trans* isomerization (cf., Supporting Information). Starting from the most stable conformer, **t1**, Arrhenius activation energies of 17.3 – 18.5 kcal/mol were calculated for these processes (which translate into unimolecular rate constants of 0.4 – 3.3 s^{-1} at room temperature, assuming zero activation entropies).

As a byproduct of the above calculations, we also obtained the full IR spectra of all conformers of **6** and **10**, some of which

(28) The dissociation of neutral COCl is slightly endothermic (Nicovitch, J. M.; Kreutter, P. H.; Wine, P. H. *J. Chem. Phys.* **1990**, *92*, 3539.), whereas the COCl anion decays spontaneously to $\text{CO} + \text{Cl}^-$ (Karpas, Z.; Klein, F. S. *Int. J. Mass Spectrom. Ion Phys.* **1976**, *22*, 189).

(27) Schnöckel, H.; Eberlein, R. A.; Plitt, H. S. *J. Chem. Phys.* **1992**, *97*.

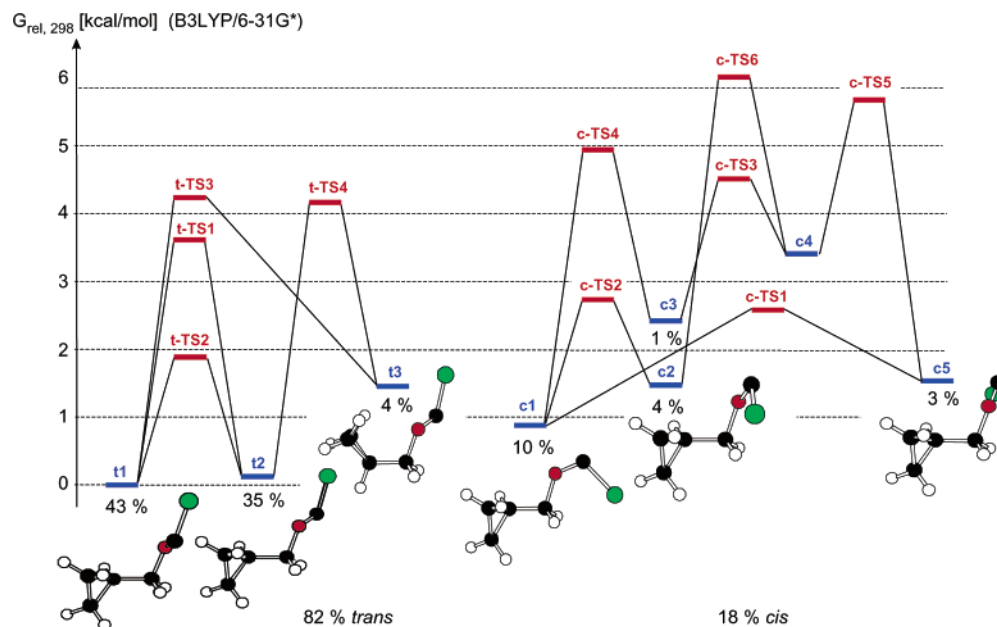


Figure 3. Different conformers of oxychlorocarbene **6** (blue bars) and transition states for their interconversion (red bars), shown on a free energy scale computed by the B3LYP/6-31G* method. Percentages in an equilibrium mixture at 298 K are indicated below the blue bars.

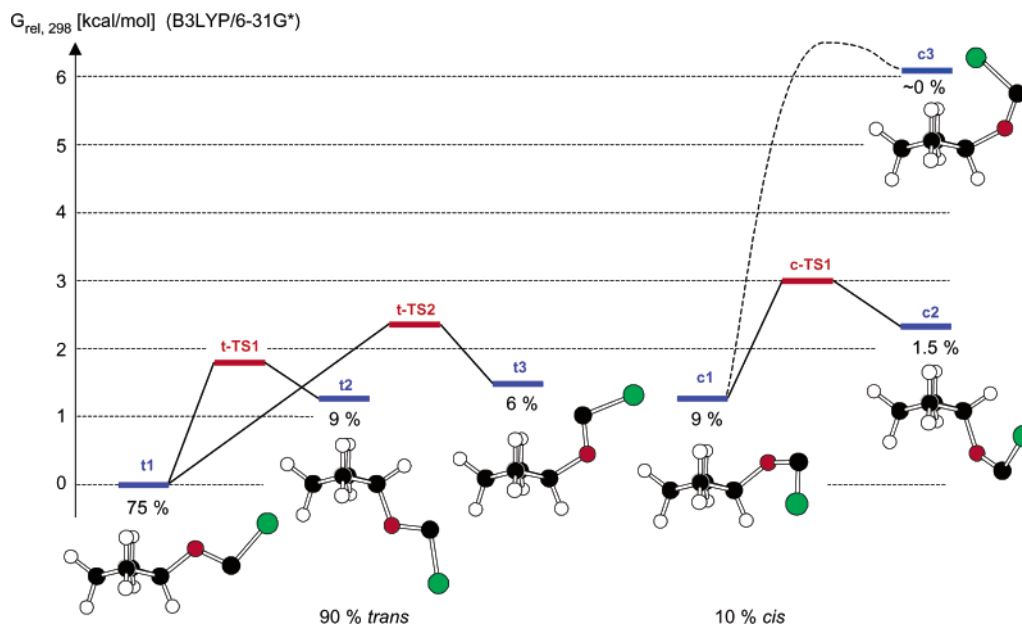


Figure 4. Different conformers of oxychlorocarbene **10** (blue bars) and transition states for their interconversion (red bars), shown on a free energy scale computed by the B3LYP/6-31G* method. Percentages in an equilibrium mixture at 298 K are indicated below the blue bars.

are displayed at the top and the bottom of Figure 2. The calculations predict only a single intense band in the region of 1250–1320 cm^{-1} for each conformer, whereas the experimental difference spectra show a multitude of bands in this region in both cases. This indicates the presence of multiple conformers after matrix photolysis of diazirines **14** and **15**. In particular, the presence of peaks around 1400 cm^{-1} leads to the conclusion that *cis*-conformers, which have much stronger predicted bands in this region, are also constituents of the mixture. As the calculations predict similar spectra for **6** and **10** in the 1200–1400 cm^{-1} region, the appearance of similar bands in this region cannot be taken as a proof for the formation of **6** from **15** or **10** from **14**.

Next we turned to an exploration of the different decomposition pathways depicted in Figure 5 (relative energies listed in

Table 2; for full information, see Supporting Information). Of these decompositions, the homolytic cleavage to $\text{C}_4\text{H}_7^{\bullet} + \text{COCl}^{\bullet}$ turned out to be the least favorable one, with an endothermicity of 21 kcal/mol for **6** and 25 kcal/mol for **10**, respectively. Hence, the *trans*-oxychlorocarbenes presumably undergo isomerization to the *cis*-conformers (which have low-energy fragmentation pathways available; see below) rather than suffer homolytic fragmentation, in contrast to the benzyl case where the latter pathway is the favored one for the *trans*-conformer of $\text{PhCH}_2\text{O}\ddot{\text{C}}\text{Cl}$.¹¹ It is therefore not surprising that **9**, a product which is expected to arise by ring opening of the cyclopropylmethyl radical, is a minor product in the room temperature experiments (note, however, that some **9** may also arise from ionic processes involving cations **1** or **2**^{2,4}).

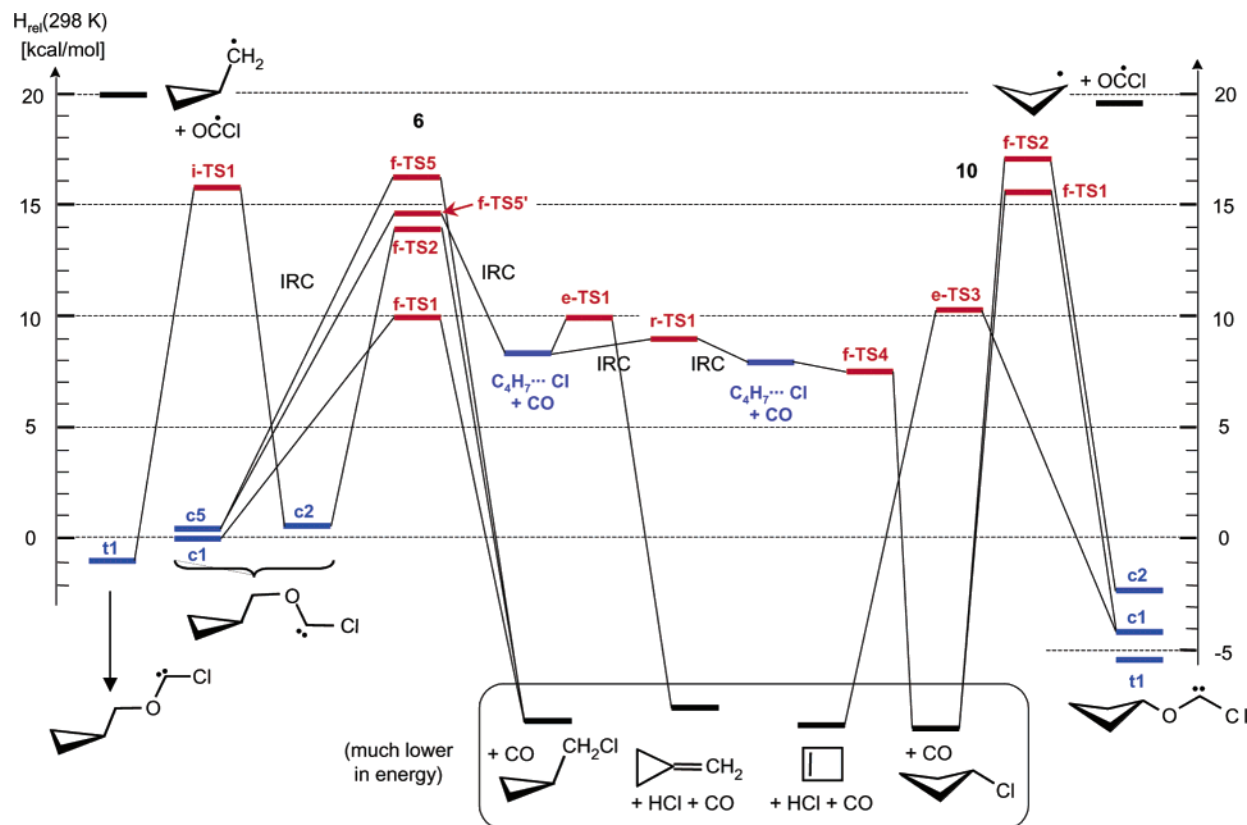


Figure 5. Decomposition pathways of oxychlorocarbenes **6** (left side) and **10** (right side), depicted on a 298 K enthalpy scale computed by the B3LYP/6-31G* method. A transition state for *trans* → *cis* interconversion of **6** is shown for reference, as are the enthalpies of the $C_4H_7^+ + COCl^*$ radicals obtained by homolytic fragmentation of **6** or **10**, respectively. Letters preceding "TS" indicate isomerization (i), fragmentation (f), elimination of HCl (e), or rearrangement (r). IRC indicates that intrinsic reaction coordinate calculations were carried out.

Table 2. Energies of Various Stationary Points on the B3LYP/6-31G* Potential Surface of C_4H_7OCCl as Depicted in Figure 5, Calculated by Different Methods

structure	relative energy ^a		
	B3LYP 6-31G*	MP2 cc-pVDZ	CCSD(T) cc-pVDZ
6-t1	-1.22	-2.12	-1.71
6-i-TS1	16.63	20.43	19.60
6-c1	(0)	(0)	(0)
6-c2	0.52	0.50	0.53
cp* + COCl^b	23.96	22.63	23.29
6-c5	0.28	0.13	0.21
6-f-TS1	11.67	16.22	16.26
6-f-TS2	16.03	20.35	20.78
6-f-TS5'	16.61	23.10	22.57
6-f-TS5	18.06	8.00	22.54
ion pair 1	10.27	6.33	8.27
e-TS1	13.25	13.75	13.23
r-TS1	11.16	4.49	7.39
ion pair 2	9.41	1.50	5.22
f-TS4	9.76	4.66	6.99
10-e-TS3	12.51	17.64	15.28
10-f-TS1	17.40	16.40	17.89
cb* + COCl^c	23.37	23.50	22.89
10-f-TS2	19.24	24.34	22.36
10-c1	-4.36	-4.99	-5.74
10-c2	-2.91	-2.98	-4.00
10-t1	-5.77	-6.46	-6.89

^a Energies relative to **6-c1**. ^b **cp***: cyclopropylcarbinyl radical. ^c **cb***: cyclobutyl radical.

As in the previously explored cases^{9,11,29,30} and in agreement with our earlier study on C_4H_7OCCl ,⁷ we found that the *cis*-conformers can undergo concerted fragmentation to $C_4H_7Cl + CO$

Starting from the two lowest energy *cis*-conformers of oxychlorocarbene **6** (**c1** and **c2**), we found two transition states for concerted fragmentation to $C_4H_7Cl + CO$ which both lie, however, well below the lowest transition state for *trans* → *cis* isomerization (**i-TS1** in Figure 5). Thus, under conditions where there is enough energy to surmount that barrier, decomposition to $C_4H_7Cl + CO$ ensues rapidly.

Starting from **6-c5**, we found two transition states. The first of these (**f-TS5**) leads also directly to elimination of CO and collapse to C_4H_7Cl , but an IRC calculation starting from the other lower lying one (**f-TS5'**) led us eventually to a potential energy minimum that corresponds to a $C_4H_7^{\delta+} \cdots Cl^{\delta-}$ complex containing a very loosely bound CO molecule on the side. An analysis of the atomic charges according to the CHelpG scheme³¹ revealed that the charge separation δ amounts to over 0.7; i.e., this complex, which is a shallow minimum, *must be regarded as an ion pair, even in the gas phase*.

This species, which is depicted in Figure 6 ("ion pair 1"), has some noteworthy structural features: first, the Cl atom is clearly H-bonded to two of the hydrogen atoms of the C_4H_7 fragment. Second, the C–C bond above the Cl atom is significantly lengthened over that in free $C_4H_7^+$ (shown at the bottom of Figure 6) which indicates that the species may be on the way to rearrange to the cyclobutyl cation. Indeed, stepwise distortion of the geometry in this sense leads to a transition state (**r-ts1**) which very much resembles that for the $C_4H_7^+$

(29) Yan, S.; Sauers, R. R.; Moss, R. A. *Org. Lett.* **1999**, *1*, 1603.

(30) Moss, R. A.; Zheng, F.; Sauers, R. R.; Toscano, J. P. *J. Am. Chem. Soc.* **2001**, *123*, 8109.

(31) Breneman, C. M.; Wiberg, K. B. *J. Comput. Chem.* **1990**, *11*, 361.

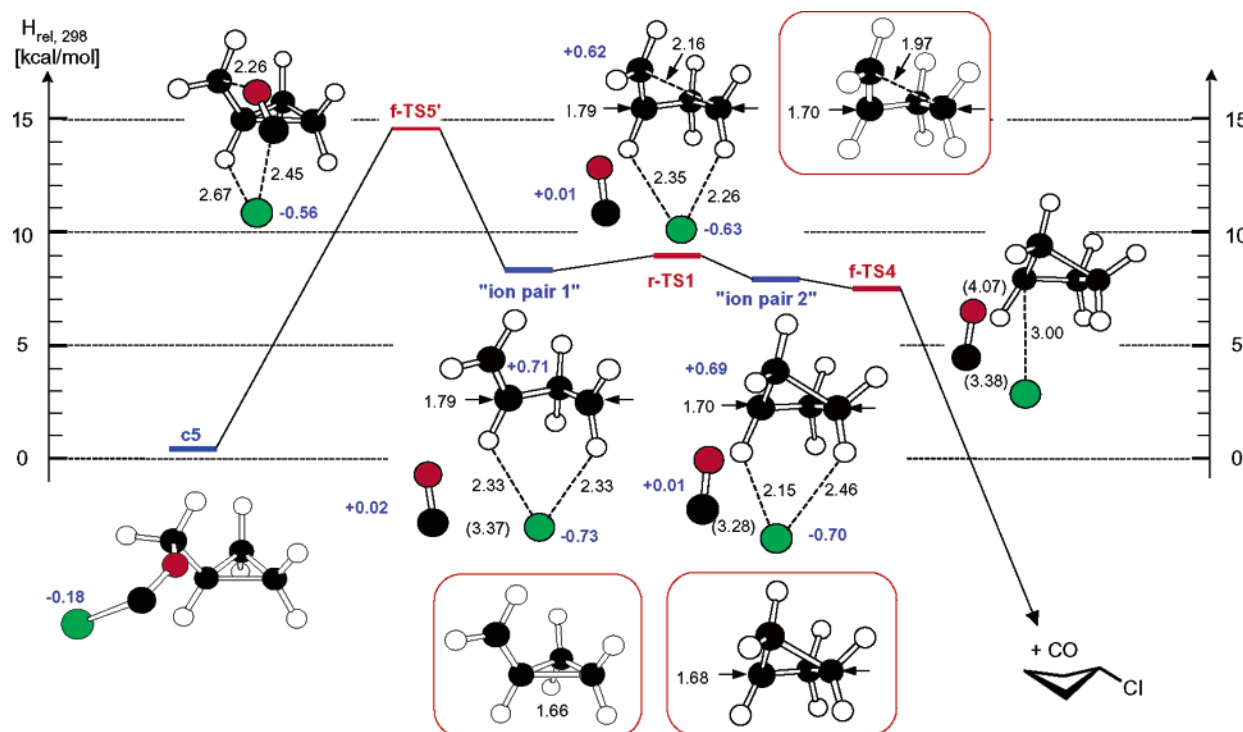


Figure 6. Pathway for fragmentation of **6** involving a rearrangement of the intermediary $C_4H_7^{\delta+}\cdots Cl^{\delta-}$ complex. Blue numbers indicate atomic charges computed by the CHelpG scheme; black numbers indicate distances between partially bonded atoms. In the red squares, the corresponding structures of the free cyclopropylcarbinyl and the cyclobutonium cations, as well as the transition state for their interconversion, calculated also at the B3LYP/6-31G* level are shown for comparison.

rearrangement (also shown in Figure 6), except that the Cl atom remains bonded to the same two hydrogen atoms as it was in the original complex. A forward IRC calculation led to a new ion pair complex where the C_4H_7 fragment now has the cyclobutyl cation structure ("ion pair 2"). This new complex is, however, only of marginal stability, as the slightest displacement of the Cl atom from its H-bonded position leads to its collapse to $C_4H_7Cl + CO$ via a "transition state" (**f-ts4**) which actually lies below the ion pair on an enthalpy scale. In contrast, the lowest energy decay path for ion pair 1, where the Cl atom is ill positioned to attack the exocyclic CH_2 group to produce **7**, is HCl elimination (see Figure 5). The structures and relative energies of both ion pairs and the transition state connecting them is insensitive to the presence or absence of the almost unbound CO.

The finding of these two ion pair complexes prompted us to search for other such structures and, in particular, for a path for formation of ion pair 2 from **10**, to explain the formation of **7** from **10**. IRC calculations on the far side of the different transition states for concerted fragmentation of carbenes **6** and **10** (**f-TS1-5**), which are already quite polar ($\delta^+/\delta^- = 0.5-0.6$), led indeed invariably to very flat regions of the potential surface representing species with a high degree of $C_4H_7^{\delta+}\cdots Cl^{\delta-}$ charge separation ($\delta^+/\delta^- = 0.7-0.8$), but all of these complexes collapsed eventually to $C_4H_7Cl + CO$ without transiting through potential energy minima. Because the fate of reactants on such flat energy surfaces depends to a large degree on nonstatistical dynamics of reactions,³² it is very possible that trajectories originating from any fragmentation transition state could also lead to rearrangements reminiscent of that which prevails in

the fluxional $C_4H_7^+$ cation,³³ thus explaining the considerable amount of "crossover" that was experimentally observed (cf. Table 1).

To ensure that these ion pair complexes are not artifacts of the B3LYP DFT model, we repeated the calculations of the two ion pairs and the transition state for their interconversion shown in Figure 6 at the MP2 and QCISD levels. Indeed the same stationary points could be located by both methods (whereby their relative energies change slightly, depending on the method; cf. Supporting Information), and the degree of CHelpG charge separation was even more pronounced (0.80–0.84) than by B3LYP at the two correlated levels. We also checked for the stability of the restricted wave functions and found that they show no tendency to form different orbitals for electrons of different spin. This finding, and the fact that the lowest triplet states of the two ion pairs are predicted to lie several eV above the closed-shell ground states, indicates that the ion pairs have no biradical character, in contrast to the case of benzyloxycarbene, where this was found to be the case.¹¹

Due to the extreme flatness of the potential energy surface for the $C_4H_7^{\delta+}$ rearrangement within the ion pair complex, many structures along the reaction path may have finite lifetimes. If a $Cl^{\delta-}$ attacks the CH_2 group to the right side of the ion pair 1 or **r-TS1** in Figure 5, this might result in cleavage of both of the weak C–C bonds and direct formation of 3-butenyl chloride **9**. Perhaps this mechanism can explain the observation of this product (Table 1), although we were not able to locate a corresponding reaction pathway.

(32) Carpenter, B. K. *Angew. Chem., Int. Ed.* **1999**, *37*, 3341.

(33) Casanova, J.; Kent, D. R.; Goddard, W. A.; Roberts, J. D. R. *Proc. Natl. Acad. Sci. U.S.A.* **2003**, *100*, 15.

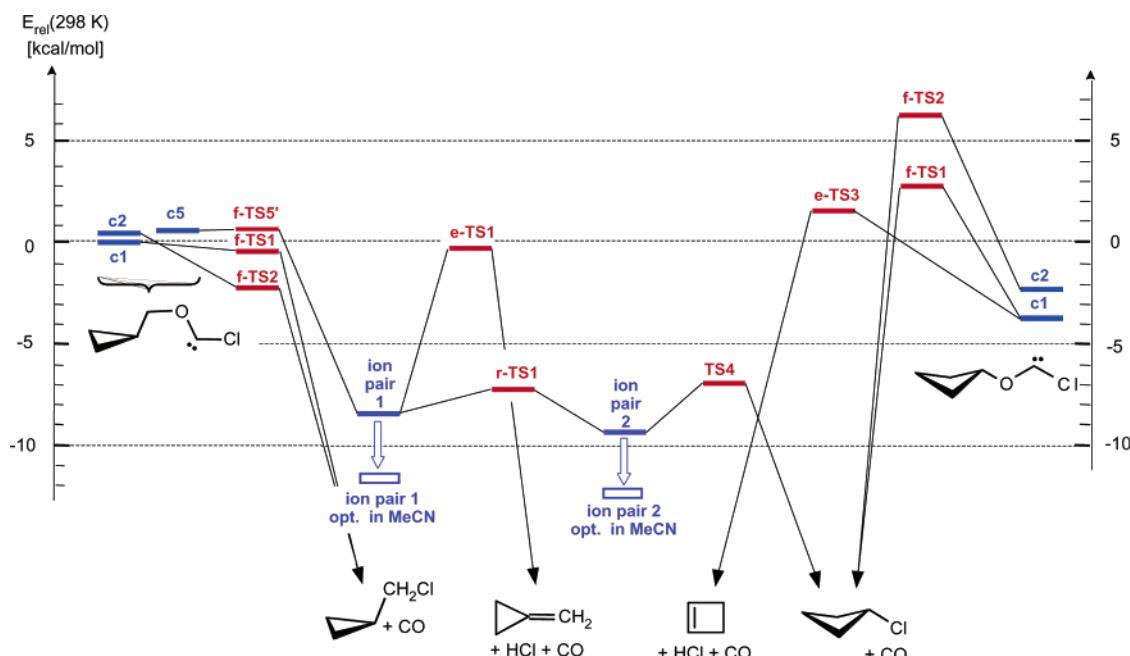


Figure 7. Energies of some stationary points from Figure 5 after single-point calculation in simulated MeCN according to the PCM procedure by B3LYP/6-31G*. Open blue bars indicate energies of the two ion pair complexes after reoptimization in MeCN.

If we turn to **10**, we note that the barriers for fragmentation to $C_4H_7Cl + CO$ are generally higher than those for the corresponding processes in **6** (we only show the two lowest lying transition states in Figure 5), but they are still lower than the barrier for homolytic cleavage to $C_4H_7^* + \cdot COCl$ and the lowest trans \rightarrow cis isomerization barriers. However, in contrast to **6**, the most favorable decay path of **10** corresponds, as in some other alkoxychlorocarbenes,¹¹ to concerted elimination of CO and HCl, leaving behind cyclobutene. When diazirine **15** was decomposed thermally in cyclohexane- d_{12} , $CDCl_3$, and CD_3CN , careful NMR analyses at 300 and 400 MHz revealed 6.6%, 1.8%, and 2.5% of cyclobutene (δ 5.97, $=CH$, 2.57, CH_2), respectively. Cyclobutene is therefore indeed a minor product, but its fraction is certainly not compatible with the B3LYP/6-31G* predictions.

In an effort to elucidate the reason for this discrepancy, we carried out single-point MP2 and CCSD(T) calculations with Dunning's cc-pVDZ basis set at the geometries of the B3LYP stationary points of all the species represented in Figure 5. The results of these calculations (Table 2) reveal that the relative energies of several of the species involved in the different $C_4H_7O\dot{C}Cl$ conversions vary by several kcal/mol between different methods. In particular, the CCSD(T) and MP2 activation barriers for fragmentation of **6** are predicted to be higher than those obtained from B3LYP calculations by 4–6 kcal/mol, and they are much closer to the energy for homolytic dissociation to $C_3H_5CH_2^* + \cdot COCl$. The effect is less pronounced on the side of **10**, but as the barrier for elimination of HCl+CO increases by 3–5 kcal/mol whereas the lowest one for fragmentations remains unchanged (or decreases by 1 kcal/mol at the MP2 level), the two processes are predicted to be much more competitive at the MP2 and CCSD(T) level ($\Delta\Delta E^\ddagger = 4.9$ kcal/mol in favor of elimination by B3LYP vs 1.24 kcal/mol in favor of fragmentation by MP2, CCSD(T) lying between), in accord with experiment.

Interestingly, the thermochemistry of the C_4H_7 rearrangement within the ion pair complex, which is nearly thermoneutral by

B3LYP, becomes exothermic in favor of the cyclobutyl species by almost 3 kcal/mol by CCSD(T) and by nearly 5 kcal/mol by MP2 (4 kcal/mol if geometries are reoptimized). This prediction is at variance with the finding that C_4H_7 "crossover" is more efficient from the side of **10** (to yield 50–60% of **7**) than from the side of **6** (where the yield of **8** is only 10–20%) which indicates that no single level of theory appears to be capable of modeling all aspects of the complex potential energy surface on which the different $C_4H_7O\dot{C}Cl$ conversions take place with equal accuracy.

B. Condensed Phase: The significant amount of charge separation that prevails already at the transition states for concerted fragmentation to $C_4H_7Cl + CO$, and of course in the ion pair complexes, suggests that these species will be stabilized relative to the oxychlorocarbenes **6** and **10** (where the charge separation is much less pronounced), if the reaction is carried out in a polar solvent. To probe this effect, we carried out calculations where such a solvent was modeled as a polarizable continuum (PCM³⁴).

The results that were obtained by single-point self-consistent reaction field (SCRF) PCM calculations in MeCN ($\epsilon = 36.6$) are shown in Figure 7. The changes from the situation that prevails in the gas phase (cf. Figure 5) are evident and dramatic: the ion pair complexes which were ca. 8 kcal/mol above the most stable *cis*-conformer of **6** lie below this oxychlorocarbene by a similar amount in MeCN. Reoptimization of the two ion pair complexes in MeCN led to a further stabilization by about 3 kcal/mol whereby the Cl anion (which now carries a charge of almost 0.9) moved about 0.4 Å away from the two H atoms to which it is bonded, and from the CO molecule, while the structure of the hydrocarbon fragment was barely affected. It is, however, noteworthy that the separated $C_4H_7^+$ cation (optimized in MeCN) + $Cl^- + CO$, all in MeCN, still lies about 2 kcal/mol above the two ion pair complexes,

(34) Amovilla, C.; Barone, V.; Cammi, R.; Cancès, E.; Cossi, M.; Mennucci, B.; Pomelli, C. S.; Tomasi, J. *Int. J. Quantum Chem.* **1999**, *32*, 227.

presumably due to hydrogen bonding of the Cl anion to the hydrocarbon fragment in the complex.

More surprisingly, the transition states for fragmentation to $C_4H_7Cl + CO$ (one of which leads to the ion pair) were also stabilized in MeCN to the point where they lie *below* the oxchlorocarbenes on the side of **6**. This finding raises the question whether the *cis*-conformers of **6** have any lifetime at all in this solvent. To answer this question would have required a reoptimization of these transition states in MeCN, an undertaking which unfortunately proved impossible with the current PCM code. However, we succeeded to reoptimize one of the transition states (and the associated reactant and product) with the self-consistent isodensity (SCI) PCM method³⁵ as implemented in Gaussian98.⁴⁴ Single-point PCM calculations on these points in acetonitrile revealed a residual barrier for the decay of **6(c2)** via **6(f-ts2)** of 1.5 kcal/mol. On the side of **10**, the conformer **c1** and the transition state **f-ts1** were optimized, which resulted in a fragmentation barrier of 4.6 kcal/mol. Thus, small barriers appear to remain, even in acetonitrile, but it is to be expected that the *cis*-conformers of the $C_4H_7O\dot{C}Cl$ are only very fleeting transients in polar solvents.

The above-mentioned technical problems also prevented us from investigating what happens to the transition state for interconversion of the two ion pairs in polar solvents.³⁶ We would, however, assume that this barrier cannot be much higher than in the free $C_4H_7^+$ cations, where it is so small that it has so far eluded experimental determination.³⁷ Interestingly, the barrier for elimination of HCl from ion pair **1** enjoys less stabilization in MeCN so that this process is no longer competitive in polar solvents, in accord with experimental findings.

An experimental finding that remains to be explained is the deuterium scrambling which was observed in chlorides **7** and **8** after photolysis of **14- α,α - d_2** . In this context, it is worth recalling that a single rearrangement pass of the α,α - d_2 -cyclopropylcarbinyl cation, **16**, leads to the β,β - d_2 -cyclobutonium cation, **17**, and that a second pass is needed to arrive at ring-deuterated cyclopropylcarbinyl cation **18**. Formation of γ,γ - d_2 -cyclobutonium **19** requires yet another passage over the transition state separating the two cations (see Figure 8). According to all experimental³⁷ and computational evidence,^{33,36} this scrambling is expected to be inherently extremely rapid, yet it apparently does not reach completion during the fragmentation of the C_4H_7 oxchlorocarbenes. This must be due to the fact that collapse to $C_4H_7Cl + CO$ is in constant competition with the above rearrangements, irrespective of the solvent in which the reaction is carried out. However, the finding of chlorides derived from **18** and **19** in the product mixture proves that at least some of the ion pairs survive long enough to effect several passes over the barrier separating the two structures before internal trapping of the hydrocarbon cation by Cl^- occurs.

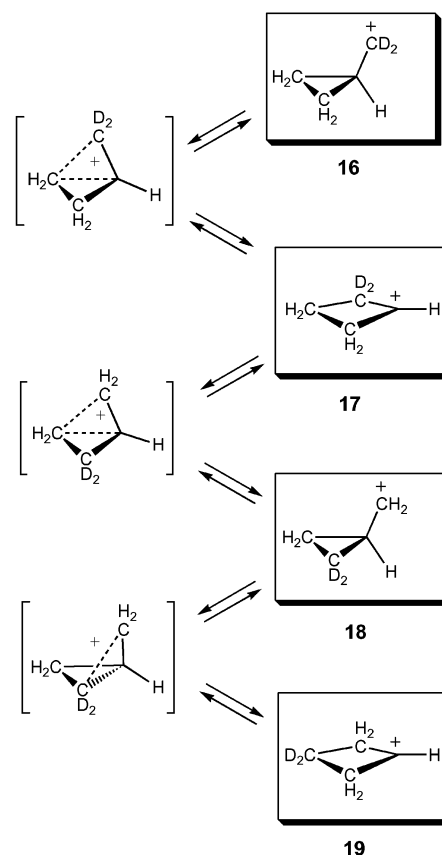


Figure 8. Interconversion of labeled $C_4H_7^+$ cations, starting from the α,α - d_2 -cyclopropylcarbinyl cation.

Conclusions

The present study reveals a remarkable new facet of the intriguing chemistry of oxchlorocarbenes $RO\dot{C}Cl$: apparently the charge separation between the hydrocarbon fragment R and the Cl atom with which it eventually recombines can be sufficiently pronounced that rearrangements typical of free carbocations may occur, even in nonpolar solvents (or in the gas phase¹⁷). According to DFT and correlated post-HF calculations, these $R^{\delta+}\cdots Cl^{\delta-}$ complexes may even appear in the form of metastable intermediates, i.e., ion pairs. These intermediates exist only in conformations where the Cl atom is hydrogen-bonded to the most acidic hydrogen atoms in the hydrocarbon fragments, and they appear to owe their marginal persistence to this factor. However, rearrangements can only occur within these complexes if they involve negligible barriers; otherwise collapse to RCl will prevent them from occurring. Indeed, product distributions and the partial scrambling of isotopic labels show that full equilibration of the C_4H_7 moiety is not achieved within its complex with Cl.

The finding of these $R^{\delta+}\cdots Cl^{\delta-}$ complexes leads to the questions (a) what causes and (b) what “pays” for the charge separation in these species? Question (a) may be addressed in the context of recent work which has demonstrated that reactions expected to follow a radical pathway (the photodissociation of cyclopropyl iodide³⁸ or the quenching of excited azoalkanes by hydrogen atom donors³⁹) may actually involve electron-transfer

(35) Foresman, J. B.; Keith, T. A.; Wiberg, K. B.; Snoonian, J.; Frisch, M. J. *J. Phys. Chem.* **1996**, *100*, 16098.

(36) We have subjected the $C_4H_7^+$ cations and the transition state for their interconversion to optimization and frequency calculations at the QCSID/6-31G* level followed by single-point calculations at the CCSD(T)/cc-pVTZ level. On inclusion of ZPE differences, the cyclobutonium cation is less stable than the cyclopropylcarbinyl cation by 0.1 kcal/mol, while the activation enthalpy (starting from the latter cation) is 0.62 kcal/mol. (On a 298 K enthalpy scale, the transition state falls 0.22 kcal/mol *below* the cyclopropylcarbinyl cation!) Thus, at this level of theory, the system must be regarded as extremely fluxional, perhaps nonclassical, in the gas phase.

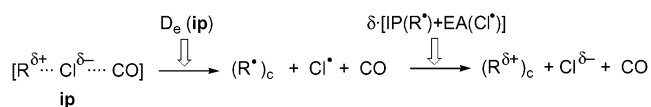
(37) Cacace, F.; Chiavarino, B.; Crestoni, M. E. *Chem.—Eur. J.* **2000**, *6*, 2024 and references therein.

(38) Arnold, P. A.; Cosofret, B. R.; Dylewski, S. M.; Houston, P. L.; Carpenter, B. K. *J. Phys. Chem. A* **2001**, *105*, 1693.

(39) Sinicropi, A.; Pogni, R.; Basosi, R.; Robb, M. A.; Gramlich, G.; Nau, W. M.; Olivucci, M. *Angew. Chem., Int. Ed.* **2001**, *40*, 4185.

steps, i.e., access ion pair complexes of the kind we have encountered in the present work. In the above cited cases, it was shown by calculations that the electron transfers are mediated by crossings from diradical to ion pair state surfaces and back. We suggest that the decay of oxychlorocarbenes involves similar surface crossings: when CO pulls away from *cis*-RO \ddot{C} Cl, the surface leading to $R^{\bullet} + Cl^{\bullet} + CO$ crosses that of a charge-transfer excited state which touches bottom at geometries where the $Cl^{\delta-}$ is hydrogen bonded to the $R^{\delta+}$ moiety. On removing the $Cl^{\delta-}$ from this position (e.g., by increasing the $R^{\bullet}\cdots Cl$ distance), the diradical surface again falls below the ionic one and back electron transfer takes place, followed by collapse to RCl. A computational exploration of these potential surfaces (which requires multideterminantal methods and the location of conical intersections) lies beyond the scope of the present work and must be left to a future study. However, the present example may well be the first documented case of a *thermal* reaction that involves such multiple crossings of diradical and ion pair surfaces, and the first case where such ion pairs correspond to potential energy minima, even in the gas phase. Analogous to the photodissociation of cyclopropyl iodide, where the finding of allyl radicals points toward the involvement of ionic species,³⁸ it is a cationic rearrangement which provides evidence for the intermediacy of ion pairs in the present case.

To shed some light on question (b), above we calculated the following (hypothetical) reaction:



where the subscript “c” indicates that the energies of the radical R^{\bullet} and the cation $R^{\delta+}$ are evaluated at the geometry of the R moiety in the ion pair complex. The overall energy change for the above reaction was calculated to be 82.7 kcal/mol for ion pair 1 and 92.9 kcal/mol for ion pair 2 in Figure 5 (using the experimental value of 3.6 eV for $EA(Cl^{\bullet})$ and the CHelpG values for the charge separation, δ). An estimation of the electrostatic attraction between $R^{\delta+}$ and $Cl^{\delta-}$ in the ion pairs was obtained by summing over all pairwise interactions between atoms, using CHelpG charges and the B3LYP interatomic distances. According to this Madelung-type procedure, Coulombic attraction amounts to 38.1 kcal/mol in ion pair 1 and to 41.3 kcal/mol in ion pair 2.⁴⁰ Thus, 44.5 or 52.9 kcal/mol, respectively, remain to be accounted for by hydrogen bonding and other stabilizing interactions whose origin is, however, presently unclear to us.

Of course, once these strongly dipolar species are placed in a dielectric continuum of sufficient permittivity, they will be effectively stabilized relative to the starting oxychlorocarbenes. According to our calculations, this stabilization leads to an almost complete disappearance of the barriers for the decay of the *cis*-conformers of the $C_4H_7O\ddot{C}Cl$ to $C_4H_7Cl + CO$. Hence the *cis*-conformers can be no more than very fleeting intermediates in polar solvents. Since the activation energy for *trans* \rightarrow *cis* isomerization is smaller than the endothermicity of homolytic cleavage, the lifetime of the incipient oxychlorocarbene should

be limited by the rate of the former process (both in the gas phase and in polar solvents).

Formation of acid chlorides RCOCl requires homolysis, a process which cannot be achieved thermally, but is possible photochemically as demonstrated by the appearance of C_4H_7COCl in the matrix experiments. However, in contrast to the benzyl case,¹¹ where free radicals were observed, the incipient $R^{\bullet}\cdots OC^{\bullet}Cl$ radical pair here appears to collapse immediately, back to RO $\ddot{C}Cl$ or to RCOCl.

Experimental and Computational Methods Section

Cyclobutylisouronium Trifluoromethanesulfonate (13). This material was prepared¹⁸ from cyclobutanol.⁴¹ In a 50 mL round-bottom flask, equipped with a reflux condenser protected with a $CaCl_2$ tube, were placed 0.73 g (17.4 mmol) of cyanamide, 5.0 g (69.4 mmol) of cyclobutanol, and 10 mL of dry THF. To this solution was added 1.67 g (17.4 mmol) of trifluoromethanesulfonic acid. The mixture was stirred magnetically at 25 °C for 30 h. Then it was diluted with 200 mL of ether and chilled in the refrigerator. A light brown oil formed which crystallized after a week at room temperature. The white crystals of **13** were washed with ether and dried in vacuo, mp 69–70 °C. ¹H NMR (δ , DMSO-*d*₆): 8.30 (br s, 4 H, 2NH₂), 4.93 (m, 1H, CHO), 2.46, 2.07, 1.80, 1.54 (m's, 6 H, cyclobutyl). The yield of **13** was 9.8 g (54%). Anal. Calcd for $C_6H_{11}F_3N_2O_4S$: C, 27.3; H, 4.2; N, 10.6. Found: C, 27.3; H, 4.3; N, 10.6.

Cyclopropylmethylisouronium Methanesulfonate (12). This oily material was prepared from commercially available cyclopropylmethanol as described for **13**, except that methanesulfonic acid was used instead of triflic acid. The isouronium salt has been characterized as the crystalline tosylate (mp 117–119 °C), using toluenesulfonic acid in a similar procedure.⁴² ¹H NMR (δ , DMSO-*d*₆): 8.40 (br s, 4 H, 2NH₂), 7.30 (center of A_2B_2 q, 4 H, aromatic), 4.07 (d, $J = 6$ Hz, OCH₂), 2.27 (s, 3 H, CH₃), 1.20 (m, 1 H, cyclopropyl CH), 0.60 (m, 2 H, cyclopropyl), 0.33 (m, 2 H, cyclopropyl). Anal. Calcd for $C_{12}H_{18}N_2O_4S$: C, 50.3; H, 6.3; N, 9.8. Found: C, 50.0; H, 6.4, N, 10.0.

3-Chloro-3-cyclobutoxydiazirine (15). The general procedure of Graham¹⁹ was followed. To 3.5 g of LiCl in 50 mL of DMSO was added 1.0 g (3.8 mmol) of isouronium salt **13** and 50 mL of pentane. The mixture was stirred magnetically and cooled to 20 °C. Then 200 mL of 12% aqueous sodium hypochlorite (“pool chlorine”), saturated with NaCl, was slowly added. After addition was complete, stirring was continued for 15 min at 15 °C. The reaction mixture was transferred to a separatory funnel containing 150 mL of ice water, the aqueous phase was removed, and the pentane phase was washed twice with 75 mL portions of ice water and then dried for 2 h over $CaCl_2$ at 0 °C. The pentane solution of diazirine **15** was purified by chromatography over 200–400 mesh 60 Å silica gel eluted with pentane. Pentane was reduced by rotary evaporation and replaced with 30 mL of DCE, MeCN, or cyclohexane-*d*₁₂, as desired. Residual pentane was then removed by rotary evaporation at 0 °C. ¹H NMR (δ , CD₃CN): 4.2–4.4 (m, 1 H, CHO), 1.5–1.8 1.2–1.5 (m, 6 H, cyclobutyl). UV (λ_{max} , nm): 352, 367 (pentane), 353, 367 (DCE), 355, 369 (MeCN).

3-Chloro-3-cyclopropylmethoxydiazirine (14). This diazirine was similarly prepared from isouronium salt **12**. ¹H NMR (δ , CDCl₃): 3.74 (d, 2 H $J = 7.6$ Hz, CH₂O), 1.10 (m, 1 H, ring CH), 0.63 (m, 2H, cyclopropyl), 0.31 (M, 2 H, cyclopropyl). UV (λ_{max} , nm): 352, 368 (pentane), 354, 368 (DCE), 355, 369 (MeCN).

For **14- α,α -d₂**, cyclopropylmethanol- α,α -d₂ was prepared by the LiAlH₄ reduction of methyl cyclopropanecarboxylate in ether. This alcohol was converted to the labeled diazirine as described above, via

(40) These values are not unreasonable: they correspond to the electrostatic attraction between two point charges of 0.7 at a distance of ca. 4.3 Å which is not far from the distance of the Cl atom from the center of charge of the cationic hydrocarbon moieties in the two ion pair complexes.

(41) Lee, C. C.; Cessna, A. *Can. J. Chem.* **1980**, *58*, 1075.

(42) Ho, G.-J. PhD Dissertation, Rutgers University, 1992.

12- α,α - d_2 . The ^1H NMR spectrum of 14- α,α - d_2 was identical to that of 14, except for the absence of the α - CH_2 doublet at δ 3.74.

Products. Authentic chlorides 7 and 8 were commercially available. 1-Chloro-3-butene was prepared from 3-buten-1-ol with thionyl chloride and pyridine.⁴³

Photolysis of Diazirines. Solutions of diazirines 14 or 15 in pentane, DCE, or MeCN ($A = 1.0$ at λ_{max}) were irradiated for 1 h with a focused UV lamp, $\lambda > 320$ nm (uranium glass filter). The products were analyzed by capillary GC and GC-MS using a $30\text{ m} \times 0.25\text{ mm}$ (o.d.) $\times 0.25\ \mu\text{m}$ (i.d.) CP-Sil 5CB (100% dimethyl polysiloxane) column at 25 °C (4 min, programmed to 80 °C at 10 deg/min). The products and distributions are described above. Their identities were confirmed by GC and GC-MS comparisons to authentic materials.

Matrix Isolation and Spectroscopy.⁴⁴ A few milliliters of cold pentane solutions of diazirines 14 or 15 were placed in a U-shaped tube connected to the inlet system of a closed-cycle cryostat and immersed in a constant-temperature bath. While the bath was kept at -70 °C, the pentane was pumped off, leaving a dry film of diazirine on the walls of the U-tube. While the tube was kept at -70 °C, the valves toward the spray-on line and the cryostat were opened. Then the temperature of the bath was increased to -45 °C, whereupon the diazirine was slowly entrained with the 10:1 Ar/N₂ mixture flowing over it at ca. 3 mmol/h. After about 2 h, a homogeneous matrix containing ca. 5 μmol of diazirine was formed. Electronic absorption (EA) spectra were taken between 200 and 1000 nm with a Perkin-Elmer Lambda 19 instrument, whereas IR spectra were obtained on a Bomem DA3 interferometer (1 cm^{-1} resolution) equipped with an MCT detector (500–4000 cm^{-1}). Photolyses were carried out with a high-pressure Hg/Xe lamp using cutoff or interference filters for wavelength selection, as indicated in the text.

Quantum Chemical Calculations. The geometries of all species were optimized by the B3LYP density functional method^{45,46} as implemented in the Gaussian98 program package,^{47,48} using the 6-31G* basis set. All stationary points (minima, transition states) were characterized by second derivative calculations which served also for the calculation of vibrational spectra. Radicals were calculated on the basis of densities modeled by spin-unrestricted wave functions.⁴⁹

Calculations in solution (single-point at the gas-phase geometries) were carried out by the polarized continuum model (PCM)³⁴ within the self-consistent reaction field (SCRF) procedure as implemented in Gaussian 03,⁵⁰ using acetonitrile as a solvent. Reoptimization of the

geometries of the oxychlorocarbenes in this solvent did not result in significant changes or stabilizations, but unfortunately all attempts to reoptimize the ion pairs or the transition states for fragmentation with the above PCM method failed to converge. In two cases this proved, however, possible with the self-consistent isodensity (SCI) variant of the PCM method as implemented in Gaussian.³⁵

Acknowledgment. This work was supported by the U.S. National Science Foundation (CHE 0091368) and the Swiss National Science Foundation (Project No. 2000-067881.02). Access to the computational resources of the Center for Neurosciences at Rutgers University (Newark) is appreciated.

Supporting Information Available: Cartesian coordinates and energies (including enthalpies and free energies) of all stationary points discussed in this study. This material is available free of charge via the Internet at <http://pubs.acs.org>.

JA049421X

(43) Roberts, J. D.; Mazur, R. H. *J. Am. Chem. Soc.* **1951**, *73*, 2509.

(44) Bally, T. In *Reactive Intermediate Chemistry*; Moss, R. A., Platz, M. S., Jones, M., Jr., Eds.; Wiley: New York, 2003.

(45) Becke, A. D. *J. Chem. Phys.* **1993**, *98*, 5648.

(46) Lee, C.; Yang, W.; Parr, R. G. *Phys. Rev. B* **1988**, *37*, 785.

- (47) Frisch, M. J.; Trucks, G. W.; Schlegel, H. B.; Scuseria, G. E.; Robb, M. A.; Cheeseman, J. R.; Zakrzewski, V. G.; Montgomery, J. A.; Stratmann, R. E.; Burant, J. C.; Dapprich, S.; Millam, J. M.; Daniels, A. D.; Kudin, K. N.; Strain, M. C.; Farkas, O.; Tomasi, J.; Barone, V.; Cossi, M.; Cammi, R.; Mennucci, B.; Pommelli, C.; Adamo, C.; Clifford, S.; Ochterski, J.; Petersson, G. A.; Ayala, P. Y.; Cui, Q.; Morokuma, K.; Malick, D. K.; Rabuck, A. D.; Raghavachari, K.; Foresman, J. B.; Cioslowski, J.; Ortiz, J. V.; Stefanov, B. B.; Liu, G.; Liashenko, A.; Piskorz, P.; Komaromi, I.; Gomperts, R.; Martin, R. L.; Fox, D. J.; Keith, T.; Al-Laham, M. A.; Peng, C. Y.; Nanayakkara, A.; Challacombe, M.; Gill, P. M. W.; Johnson, B. G.; Chen, W.; Wong, M. W.; Andres, J. L.; Gonzales, C.; Head-Gordon, M.; Repogle, E. S.; Pople, J. A. *Gaussian 98*, rev A7-A11. Gaussian, Inc.: Pittsburgh, PA, 1998.
- (48) For a description of the DFT methods implemented in the Gaussian program, see: Johnson, B. G.; Gill, P. M. W.; Pople, J. A. *J. Chem. Phys.* **1993**, *98*, 5612.
- (49) Bally, T.; Borden, W. T. In *Reviews in Computational Chemistry*; Lipkowitz, K. B., Boyd, D. T., Eds.; Wiley-VCH: New York, 1999; Vol. 13, p 1.
- (50) Frisch, M. J.; Trucks, G. W.; Schlegel, H. B.; Scuseria, G. E.; Robb, M. A.; Cheeseman, J. R.; Montgomery, J. A.; Vreven, T.; Kudin, K. N.; Burant, J. C.; Millam, J. M.; Iyengar, S. S.; Tomasi, J.; Barone, V.; Mennucci, B.; Cossi, M.; Scalmani, G.; Rega, N.; Petersson, G. A.; Nakatsuji, H.; Hada, M.; Ehara, M.; Toyota, K.; Fukuda, R.; Hasegawa, J.; Ishida, M.; Nakajima, T.; Honda, Y.; Kitao, O.; Nakai, H.; Klene, M.; Li, X.; Knox, J. E.; Hratchian, H. P.; Cross, J. B.; Adamo, C.; Jaramillo, J.; Gomperts, R.; Stratmann, R. E.; Yazyev, O.; Austin, A. J.; Cammi, R.; Pomelli, C.; Ochterski, J. W.; Ayala, P. Y.; Morokuma, K.; Voth, G. A.; Salvador, P.; Dannenberg, J. J.; Zakrzewski, V. G.; Dapprich, S.; Daniels, A. D.; Strain, M. C.; Farkas, O.; Malick, D. K.; Rabuck, A. D.; Raghavachari, K.; Foresman, J. B.; Ortiz, J. V.; Cui, Q.; Baboul, A. G.; Clifford, S.; Cioslowski, J.; Stefanov, B. B.; Liu, G.; Liashenko, A.; Piskorz, P.; Komaromi, I.; Martin, R. L.; Fox, D. J.; Keith, T.; Al-Laham, M. A.; Peng, C. Y.; Nanayakkara, A.; Challacombe, M.; Gill, P. M. W.; Johnson, B.; Chen, W.; Wong, M. W.; Gonzalez, C.; Pople, J. A. *Gaussian 03*, Rev B.01; Gaussian, Inc.: Pittsburgh, PA, 2003.